Characterization of the Interaction of Wheat Germ Protein Synthesis Initiation Factor eIF-3 with mRNA Oligonucleotide and Cap Analogues†

Susan E. Carberry and Dixie J. Goss*
Department of Chemistry, Hunter College of the City University of New York, New York, New York 10021-5024
Received July 15, 1991; Revised Manuscript Received September 25, 1991

ABSTRACT: Direct fluorescence titration experiments of wheat germ protein synthesis initiation factor eIF-3 with mRNA cap and oligoribonucleotide analogues were performed in order to determine the equilibrium association constants (K_{eq}) for the eIF-3·mRNA interaction as a function of pH and temperature. These data suggest that (i) the eIF-3·mRNA interaction is not cap-specific (i.e., m^{7}G-specific), (ii) ATP hydrolysis is not involved in the interaction, and (iii) the interaction is primarily ionic in nature. Competition experiments between a rabbit α-globin mRNA oligoribonucleotide analogue and either mRNA cap analogues or nucleoside triphosphates (NTPs) are also reported; these experiments indicate that NTPs act as both activators and competitive inhibitors of the mRNA·eIF-3 association. The results are consistent with a partially uncompetitive binding mechanism, whereby at low NTP concentrations ($\leq$10 μM) the bound NTP enhances subsequent mRNA binding to eIF-3, perhaps by inducing a conformational change, and at higher NTP concentrations, the NTP acts as a competitive inhibitor for the mRNA binding site on eIF-3.

Wheat germ eukaryotic initiation factor 3 (eIF-3)[1] is a large protein complex consisting of 10 polypeptides ranging in size from about 28 to 116 kDa; eIF-3 has a total molecular mass of approximately 660–770 kDa (Checkley et al., 1981; Lax et al., 1986). Early studies have shown that the 28-, 87-, and 116-kDa subunits of wheat germ eIF-3 (and to a lesser extent, the 56-kDa subunit) were capable of cross-linking to the oxidized 5′-termini of viral mRNA (Sonenberg & Shatkin, 1977; Sonenberg et al., 1979). Furthermore, Setyono et al. (1984) showed that the 64-, 66-, 95-, and 110-kDa subunits of reticulocyte eIF-3 directly cross-linked to Semliki Forest viral mRNA.

Recently, Rychlik et al. (1991) have reported that a photoaffinity analogue of the mRNA cap which could cross-link to the active cap binding site on the 25-kDa cap binding protein could also be directly cross-linked to the 66-kDa subunit of eIF-3; furthermore, this cross-linking could be inhibited by m^{7}GTP. We have also reported the formation of a binary complex between wheat germ eIF-3 and either mRNA cap or oligoribonucleotide analogues (Carberry & Goss, 1991b); however, the details of the eIF-3·mRNA interaction have not been fully characterized.

In the present study, we have characterized the interaction of wheat germ eIF-3 with mRNA cap analogues, nucleoside triphosphates, and rabbit α-globin mRNA oligoribonucleotide analogues using direct fluorescence titration methods. These data indicate that the eIF-3·mRNA interaction is not cap-specific (i.e., m^{7}G-specific) and is primarily ionic in nature; ATP hydrolysis is not involved in the interaction. Competition experiments between mRNA and NTPs for binding eIF-3 suggest a partially uncompetitive mechanism whereby the NTP enhances mRNA binding, while at higher concentrations, the NTP competitively inhibits mRNA binding.

Materials and Methods

Wheat germ eIF-3 was prepared as described by Lax et al. (1986). m^{7}GTP, GTP, and ATP were purchased from Pharmacia Molecular Biologicals; ϵ-ATP was purchased from Molecular Probes, and AMP-PNP was purchased from Sigma. The rabbit α-globin mRNA oligoribonucleotide analogues (Figure 1) were prepared by cell-free transcription in a T7 RNA polymerase system according to the method of Milligan et al. (1987) and were purified according to the method of Draper et al. (1988). The ATPase activity of eIF-3 was assayed spectrophotometrically according to the procedure of Secrist et al. (1972).

The interaction of eIF-3 with mRNA analogues was measured by direct titration of eIF-3 with either cap or oligoribonucleotide analogue or with NTPs. The measurements were carried out at 23 ± 0.2 °C utilizing an excitation wavelength of 258 nm; for temperature-dependent studies, the temperature of the sample was maintained by circulating thermostated water through the fluorometer's brass cuvette holder. All solutions for fluorescence were prepared in buffer A, consisting of 20 mM HEPES and 1 mM DTT in the presence of 100 mM KCl and 2 mM $MgCl_2$, adjusted to pH 7.6, unless otherwise noted. The details of the titration protocol have been described elsewhere (Carberry et al., 1989, 1990). The samples were corrected for the small dilution during the course of the titration; an inner filter effect correction was not required over the range of oligoribonucleotide and NTP concentrations used. In brief, 0.4 μM eIF-3 was titrated with cap or mRNA analogue, and the decrease in the fluorescence intensity of eIF-3 at 330 nm was monitored; these data were used to construct Eadie–Hofstee plots, and the equilibrium association constant (K_{eq}) values were directly determined from the slopes of these plots (Carberry & Goss, 1991b). For

† This work was supported by grants from the National Science Foundation (NSF 9007807) and the American Heart Association (AHA–NYC Established Investigatorship and Grant-in-Aid) and by a PSC–CUNY Faculty Award (D.J.G.). S.E.C. is supported by an American Heart Association–NYC Postdoctoral Fellowship. This investigation was supported in part by a "Research Centers in Minority Institutions" award (RR-0307) from the Division of Resources, NIH, to Hunter College.
* Address correspondence to this author.

[1] Abbreviations: m^{7}G; 7-methylguanosine; ϵ-ATP; 1,N^6-ethenoadenosine 5′-triphosphate; AMP-PNP; 5′-adenylyl imidodiphosphate; NTP; nucleoside triphosphate; eIF; eukaryotic initiation factor; HEPES; *N*-(2-hydroxyethyl)piperazine-*N*′-2-ethanesulfonic acid; DTT; dithiothreitol; kDa; kilodalton(s).

0006-2960/92/0431-296$03.00/0

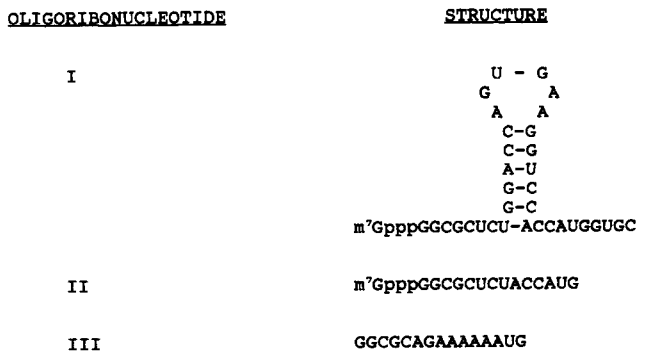

FIGURE 1: Structures of mRNA oligoribonucleotide analogues employed in this study.

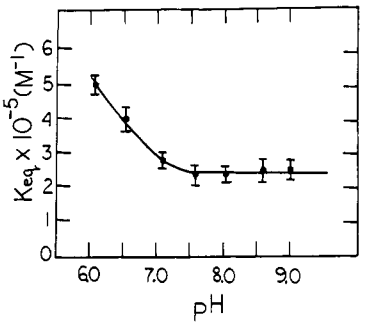

FIGURE 2: Binding of oligoribonucleotide I to eIF-3 as a function of pH. All solutions were prepared in buffer A, adjusted to the appropriate pH at 23 °C; K_{eq} values were determined as described under Materials and Methods.

titrations involving ϵ-ATP, the change in ϵ-ATP fluorescence intensity at 412 nm was also monitored and corrected for the contribution of free ϵ-ATP to the spectrum. The K_{eq} values were determined from Eadie–Hofstee plots constructed from the corrected fluorescence data.

Results

pH Dependence. The binding of wheat germ eIF-3 to oligoribonucleotide I as a function of pH is shown in Figure 2. There is a 2.2-fold decrease in the affinity of oligoribonucleotide I for eIF-3 as the pH is raised from 6.02 [K_{eq} of $(5.04 \pm 0.25) \times 10^5$ M^{-1}] to 7.6 [K_{eq} of $(2.32 \pm 0.15 \times 10^5$ M^{-1}]; as the pH is increased above 7.6, there is no further decrease in binding affinity, and the K_{eq} value remains unchanged (within experimental error). This pH-dependent binding profile suggests that eIF-3 has a single pK which is titrated by the oligoribonucleotide.

We have previously shown that the interaction of the mRNA cap-specific proteins human eIF-4E (Carberry et al., 1989, 1990) and wheat germ eIF-4F and eIF-(iso)4F (Carberry & Goss, 1991a) with cap analogues or capped mRNA oligoribonucleotides results in a biphasic pH-dependent binding profile and that this profile is due to the involvement of two pK's in the interaction: one each from the m^{7}G cap and protein. The pK of m^{7}GTP is approximately 7.4–7.8, depending upon conditions (Rhoads et al., 1983, 1985; Carberry et al., 1989). While we cannot determine the pK_a of the group(s) involved here because of the inability to perform titrations below pH 6.0, it is unlikely that the pK_a involved is that of the m^{7}G residue since the pK_a for the titration in Figure 2 is certainly below 7.0. Therefore, the single pK profile obtained for the eIF-3·oligoribonucleotide interaction suggests that the m^{7}G cap of the oligoribonucleotide is not directly involved in the formation of the binary complex.

Temperature Dependence. The temperature dependence of binding of oligoribonucleotide I to eIF-3 was measured over the 6.0–35.8 °C range. The melting of the oligoribonucleotide was not significant over this temperature range, since under the salt conditions employed (100 mM KCl, 2 mM $MgCl_2$), the T_m was found to be greater than 70 °C. The K_{eq} values obtained for the interaction of eIF-3 with oligoribonucleotide I as a function of temperature were used to construct a van't Hoff plot (data not shown). The entropy (ΔS) and enthalpy (ΔH) were determined from the intercept and slope of the plot, respectively, and were calculated to be 10.1 ± 0.5 cal/(mol·K) and -4.31 ± 0.22 kcal/mol, respectively. A positive ΔS value and a negative ΔH value are consistent with an ionic (charge neutralization) interaction (Ross & Subrmamanian, 1981).

Table I: Summary of K_{eq} Values for the Interaction of Wheat Germ eIF-3 with Cap and mRNA Oligoribonucleotide Analogues[a]

interaction	$K_{eq} \times 10^{-5}$ (M^{-1})
eIF-3·oligoribonucleotide I	2.32 ± 0.15
eIF-3·oligoribonucleotide II	4.98 ± 0.61
eIF-3·oligoribonucleotide III	4.84 ± 0.48
eIF-3·m^{7}GTP	0.40 ± 0.02
eIF-3·GTP	0.86 ± 0.08
eIF-3·ATP	0.28 ± 0.05
eIF-3·ϵ-ATP	0.45 ± 0.09
eIF-3·AMP-PNP	0.83 ± 0.05

[a] All in buffer A, pH 7.6.

Structural Dependence of Oligoribonucleotide Binding to eIF-3. In order to investigate the role of the m^{7}G cap and 5′-proximal secondary structure on the eIF-3 mRNA interaction, the binding of oligoribonucleotides II and III to eIF-3 was also measured. The capped linear oligoribonucleotide II corresponds to oligoribonucleotide I with the hairpin removed (Figure 1); the small differences in sequence were necessary in order to preserve the desired secondary structure. A comparison of the K_{eq} values for oligoribonucleotide I and II binding eIF-3 will therefore determine the relative effect of the 5′-hairpin on the interaction. Oligoribonucleotide III is an uncapped linear oligoribonucleotide (Figure 1); a comparison of the K_{eq} values for the interaction of oligoribonucleotide III and the capped linear oligoribonucleotide II with eIF-3 will provide information on the relative importance of the m^{7}G cap on the interaction.

The capped linear oligoribonucleotide II binds eIF-3 with 2.2-fold greater affinity than hairpin-containing oligoribonucleotide I (Table I). This difference may be attributed to the hairpin itself sterically reducing the surface area of the oligoribonucleotide available for contact and interaction of eIF-3. The linear oligonucleotide II lacks the steric hindrance of the hairpin, and so has more surface area available for electrostatic interactions with eIF-3, and therefore has a larger K_{eq} value for the interaction than does the hairpin-containing oligoribonucleotide II.

The effect of the m^{7}G cap on eIF-3 binding can be directly determined by comparing the K_{eq} values for the interaction of the capped linear oligoribonucleotide II and the uncapped linear oligoribonucleotide III for eIF-3. Both oligoribonucleotides have similar affinity for eIF-3 (Table I); this result suggests that the m^{7}G cap is not specifically involved in the interaction with eIF-3.

Competition Experiments between Oligoribonucleotides and the Cap Analogue or NTP for eIF-3 Binding Sites. We measured the affinity of the cap analogue m^{7}GTP and the NTPs GTP and ATP and the nonhydrolyzable analogue AMP-PNP for eIF-3, and determined how this binding affects the affinity of the rabbit α-globin mRNA oligoribonucleotide I for eIF-3. The K_{eq} values for the binding of these cofactors to eIF-3 are given in Table I. These K_{eq} values are approx-

Table II: Summary of K_{eq} and $\Delta G°_{3,MN}$ Values for the Interaction of eIF-3 and Oligoribonucleotide I in the Presence of Varying Amounts of m^{7}GTP, GTP, ATP, and AMP-PNP[a]

	m^{7}GTP		GTP		ATP		AMP-PNP	
concn (μM)	K_{eq}	$\Delta G°_{3,MN}$	K_{eq}	$\Delta G°_{3,MN}$	K_{eq}	$\Delta G°_{3,MN}$	K_{eq}	$\Delta G°_{3,MN}$
0	2.32 ± 0.15		2.32 ± 0.15		2.32 ± 0.15		2.32 ± 0.15	
2	3.17 ± 0.13	−0.18						
5	8.39 ± 0.25	−0.76	4.19 ± 0.33	−0.35	3.38 ± 0.44	−0.23	4.20 ± 0.17	−0.35
10	6.40 ± 0.83	−0.60	5.71 ± 0.21	−0.53	6.29 ± 0.25	−0.59	4.67 ± 0.59	−0.42
20	3.71 ± 0.37	−0.28	5.02 ± 0.41	−0.48	3.76 ± 0.26	−0.28	1.91 ± 0.38	+0.12

[a] All solutions in buffer A, pH 7.6; K_{eq} values are reported in 10^{-5} M^{-1}, and $\Delta G°_{3,MN}$ values are reported in kcal/mol.

imately 6–20-fold lower than the values reported for the mRNA oligoribonucleotide analogues (Table I) and are subject to greater error due to the lower relative affinity of these cofactors for eIF-3.

m^{7}GTP binds to eIF-3 with approximately 1.8-fold lower affinity than GTP. This suggests that the m^{7}G moiety does not specifically affect the mRNA·eIF-3 interaction, in agreement with the results obtained with the mRNA oligoribonucleotide analogues (Table I). ATP binds eIF-3 with approximately 3-fold lower affinity than GTP (Table I). This difference may be attributed to the differences in stacking interactions of guanosine and adenosine with aromatic amino acid residues in eIF-3, since guanosine has been shown to possess greater polarizing power than adenosine, and therefore guanosine is capable of stronger stacking interactions (Lawaczek & Wagner, 1974). The affinity of the fluorescent ATP analogue ϵ-ATP for eIF-3 was also measured. The change in fluorescence intensity of the ϵ-ATP maximum at 412 nm can be utilized to monitor the direct binding of ϵ-ATP to eIF-3. The K_{eq} value obtained from the Eadie–Hofstee plot constructed from these data reflects and binding event from the NTP perspective; if this K_{eq} value correlates with the value obtained from monitoring the change in eIF-3 fluorescence, then the same single binding event is being monitored. The K_{eq} value obtained for the ϵ-ATP eIF-3 interaction is only slightly (1.6-fold) greater than the K_{eq} value for the corresponding ATP·eIF-3 interaction obtained from protein fluorescence data. This suggests that a single binding event is being monitored. In order to further confirm this point, Scatchard plots of these data were constructed; these plots were linear, suggesting that eIF-3 possesses either a single binding site or multiple identical binding sites for NTP binding (data not shown).

The spectrophotometric method of Secrist et al. (1972) was used to monitor the ATP hydrolysis activity of eIF-3; the results of this assay showed that eIF-3 did not hydrolyze ATP. In order to confirm this result, the affinity of the nonhydrolyzable ATP analogue AMP-PNP for eIF-3 was measured. AMP-PNP was found to bind eIF-3 1.4- and 2.3-fold more strongly than ϵ-ATP and ATP, respectively (Table I); this result suggests that ATP hydrolysis is not involved in the mRNA binding process, since the values are not significantly different when the experimental error is taken into account.

Competition experiments between m^{7}GTP, GTP, ATP or AMP-PNP, and oligoribonucleotide I for eIF-3 were also performed. The K_{eq} values obtained at different NTP concentrations are plotted in Figure 3, and the values are given in Table II. At concentrations of $\leq$10 μM, all of these cofactors enhance the binding of the oligoribonucleotide to eIF-3 and then inhibit the interaction at higher concentrations (Figure 3). m^{7}GTP shows a 3.6-fold enhancement of oligoribonucleotide binding to eIF-3 at 5 μM concentration; GTP, ATP, and AMP-PNP all enhance oligoribonucleotide binding to eIF-3 (2.5-, 2.7-, and 2.0-fold, respectively), but at 10 μM concentration.

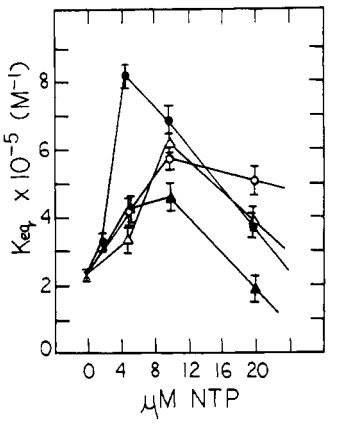

FIGURE 3: Binding of oligoribonucleotide I to eIF-3 in the presence of various concentrations of m^{7}GTP (●), GTP (○), ATP (△), and AMP-PNP (▲).

In order to determine the degree of cooperativity of the NTP, oligoribonucleotide, and eIF-3 interaction, coupling free energies were calculated according to the method of Weber (1975). The details of the calculation have been described in detail elsewhere (Goss et al., 1984, 1990; Carberry & Goss, 1991b), and the values calculated for $\Delta G°_{3,MN}$ are given in Table II. $\Delta G°_{3,MN}$ provides an estimate of how the binding of the NTP (denoted N) to eIF-3 (denoted 3) affects the subsequent binding of the oligoribonucleotide I (denoted M) to eIF-3; negative values indicate cooperative interactions while positive values reflect anticooperativity. The $\Delta G°_{3,MN}$ values obtained for these interactions are small and negative, indicating that there is a small degree of cooperativity between the NTP and oligoribonucleotide binding to eIF-3.

Lineweaver–Burk plots were constructed from the fluorescence data (data not shown). These plots all cross above the positive x axis, and are therefore diagnostic for a partially uncompetitive mechanism of interaction in which a cofactor both activates and inhibits substrate binding (Dixon & Webb, 1979). The coordinates of the crossover point for the plots of the m^{7}GTP oligoribonucleotide I·eIF-3 interaction are similar to those involving GTP, and the coordinates of the crossover point for the plots of the AMP-PNP·oligoribonucleotide I·eIF-3 interaction are similar to those involving ATP. However, the crossover points are closer to the y axis (i.e., at lower oligoribonucleotide concentrations) for the interactions involving GTP than those involving ATP, suggesting that ATP (or AMP-PNP) is a better competitive inhibitor of oligoribonucleotide binding to eIF-3 than GTP (or m^{7}GTP).

Discussion

This study has used direct fluorescence titration experiments to characterize the interaction between mRNA oligoribonucleotides and eIF-3. The thermodynamic data suggest that electrostatic interactions are primarily involved in the mRNA·eIF-3 binding. The difference in affinity of the hairpin-containing oligoribonucleotide I and linear oligoribo-

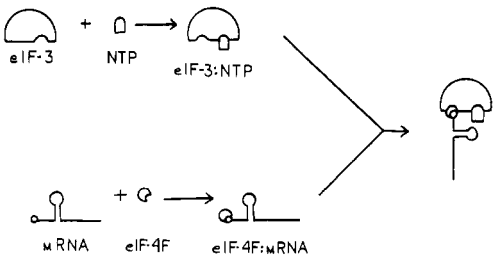

FIGURE 4: Schematic diagram for the interaction of eIF-3, eIF-4F, mRNA, and NTP. The binary mRNA·eIF-4F and eIF-3·NTP complexes combine to form a complex consisting of eIF-3, eIF-4F, mRNA, and possibly NTP.

nucleotide II may therefore be attributed to differences in the electrostatic interactions between the mRNA analogue and eIF-3: the linear oligoribonucleotide is capable of more surface contact with eIF-3 and subsequently binds more tightly than the hairpin-containing analogue. The steric bulk of the hairpin may diminish the number of contacts between the mRNA analogue and eIF-3, resulting in lower binding affinity.

Several groups have previously shown that eIF-3 can interact with the m^7G cap of mRNA (Sonenberg & Shatkin, 1977; Sonenberg et al., 1979; Setyono et al., 1984) or cross-link to mRNA photoaffinity analogues (Rychlik et al., 1991). The data presented here indicate that although eIF-3 does interact with the m^7G moiety, this interaction is not m^7G-specific: the uncapped and capped linear oligoribonucleotides both bind with equal affinity to eIF-3, with a similar trend observed for m^7GTP and GTP (Table I). Therefore, we conclude that the eIF-3·mRNA interaction is primarily *not* cap-specific.

The results of the competition experiments may be used to develop a model for the interaction of mRNA with eIF-3. The Lineweaver–Burk plots were found to be diagnostic for a partially uncompetitive mechanism of interaction [see, e.g., Dixon and Webb (1979)]. This mechanism suggests that there is a preferred *order* of interaction. At low NTP concentrations (≤ 10 μM), the NTP binds first to eIF-3; this binding process may result in conformational changes in eIF-3, which subsequently enhances the binding of the oligoribonucleotide to eIF-3. At greater NTP concentrations, the NTP can potentially fill the oligoribonucleotide binding site(s) on eIF-3 and therefore act as a competitive inhibitor of oligoribonucleotide binding, thereby decreasing the apparent K_{eq} value. Scatchard plots of the data for the various NTP eIF-3 interactions were found to be linear, indicating either that there is a *single* binding site on eIF-3 which accommodates both the NTP and the oligoribonucleotide or that there are *multiple identical* binding sites. The data presented in this study cannot distinguish between these two possibilities; however, in either case, the coupling free energies calculated from the K_{eq} data suggest that this interaction is cooperative.

The data presented here support a model which may be summarized as follows (Figure 4). First, two binary complexes form, one of which is eIF-3·NTP; the second is mRNA·eIF-4F [or mRNA·eIF-(iso)4F]. These two binary complexes then interact to form a complex of eIF-3·mRNA·eIF-4F and, possibly, NTP. This model is based on the fact that we have previously shown than the binding of eIF-4F to mRNA is likely to precede the binding of eIF-3, since the formation of the eIF-4F·mRNA complex prior to eIF-3 binding results in a 2–3-fold enhancement of eIF-3 binding (Carberry & Goss, 1991b). The binding of NTP to eIF-3, which may result in a conformational change in eIF-3, enhances the subsequent binding of the binary eIF-4F·mRNA complex to eIF-3 by 2–4-fold. Therefore, it may be concluded that the presence of the NTP assist in the binding of the mRNA to eIF-3 which, in turn, positions the mRNA for interaction with the ribosome.

REFERENCES

Carberry, S. E., & Goss, D. J. (1991a) *Biochemistry 30*, 4542–4545.

Carberry, S. E., & Goss, D. J. (1991b) *Biochemistry 30*, 6977–6982.

Carberry, S. E., Rhoads, R. E., & Goss, D. J. (1989) *Biochemistry 28*, 8078–8083.

Carberry, S. E., Darzynkiewicz, E., Stepinski, J., Tahara, S. M., Rhoads, R. E., & Goss, D. J. (1990) *Biochemistry 29*, 3337–3341.

Checkley, J. W., Cooley, L., & Ravel, J. M. (1981) *J. Biol. Chem. 256*, 1582–1586.

Dixon, M., & Webb, E. C. (1979) *Enzymes*, 3rd ed., pp 343–344, Academic Press, New York.

Draper, D. E., White, S. A., & Kean, J. M. (1988) *Methods Enzymol. 164*, 221–237.

Goss, D. J., Parkhurst, L. J., Mehta, A. M., & Wahba, A. J. (1984) *Biochemistry 23*, 6522–6529.

Goss, D. J., Carberry, S. E., Dever, T. E., Merrick, W. C., & Rhoads, R. E. (1990) *Biochemistry 29*, 5008–5012.

Lawaczek, R., & Wagner, K. G. (1974) *Biopolymers 13*, 2003–2014.

Lax, S. R., Lauer, S. J., Browning, K. S., & Ravel, J. M. (1986a) *Methods Enzymol. 118*, 109–128.

Milligan, J. F., Groebe, D. R., Witherell, G. W., & Uhlenbeck, O. C. (1987) *Nucleic Acids Res. 21*, 8783–8798.

Rhoads, R. E. (1985) *Prog. Mol. Subcell. Biol. 9*, 104–155.

Rhoads, R. E., Hellman, G. M., Remy, P., & Ebel, J.-P. (1983) *Biochemistry 22*, 6084–6088.

Ross, P. D., & Subramanian, S. (1981) *Biochemistry 20*, 3096–3102.

Rychlik, W., Nugroho, T., Yan, R., & Rhoads, R. E. (1991) *FASEB J. 5*, A807.

Secrist, J. A., Barrio, J. R., Leonard, N. J., & Weber, G. (1972) *Biochemistry 11*, 3499–3506.

Setyono, B., van Steeg, H., & Voorma, H. O. (1984) *Biochim. Biophys. Acta 782*, 242–246.

Sonenberg, N., & Shatkin, A. J. (1977) *Proc. Natl. Acad. Sci. U.S.A.* 4388–4292.

Sonenberg, N., Morgan, M. A., Testa, D., Colonno, R. J., & Shatkin, A. J. (1979) *Nucleic Acids Res. 7*, 15–29.

Weber, G. (1975) *Adv. Protein Chem. 29*, 2–78.